ISSN 1674-1056
http://cpb.iphy.ac.cn
http://iopscience.iop.org/cpb
中国物理 B
Chinese Physics
中国物理 Chinese Physics B

Coupling-induced spectral splitting for plasmonic sensing with ultra-high figure of merit

Hua Lu(陆华), Yi-Cun Fan(范奕村), Si-Qing Dai(戴思清), Dong Mao(毛东), Fa-Jun Xiao(肖发俊), Peng Li(李鹏), Jian-Lin Zhao(赵建林)

Citation: Chin. Phys. B . 2018, 27(11): 117302. **doi:** 10.1088/1674-1056/27/11/117302

Journal homepage: http://cpb.iphy.ac.cn; http://iopscience.iop.org/cpb

What follows is a list of articles you may be interested in

Gap plasmon-enhanced photoluminescence of monolayer MoS_2 in hybrid nanostructure

Le Yu(余乐), Di Liu(刘頓), Xiao-Zhuo Qi(祁晓卓), Xiao Xiong(熊霄), Lan-Tian Feng(冯兰天), Ming Li(李明), Guo-Ping Guo(郭国平), Guang-Can Guo(郭光灿), Xi-Feng Ren(任希锋)

Chin. Phys. B . 2018, 27(4): 047302. **doi:** 10.1088/1674-1056/27/4/047302

Plasmonic Mach–Zehnder interferometric sensor based on a metal–insulator–metal nanostructure

Meng Shen(沈萌), Ming Wang(王鸣), Lan Du(杜澜), Ting-Ting Pan(潘庭婷)

Chin. Phys. B . 2017, 26(7): 077301. **doi:** 10.1088/1674-1056/26/7/077301

Thermal emission properties of one-dimensional grating with different parameters

Weixin Lin(林伟新), Guozhou Li(李国洲), Qiang Li(李强), Hongjin Hu(胡宏锦), Fang Han(韩防), Fanwei Zhang(张樊伟), Lijun Wu(吴立军)

Chin. Phys. B . 2017, 26(5): 057301. **doi:** 10.1088/1674-1056/26/5/057301

Coherent and tunable radiation with power enhancement from surface plasmon polaritons

Gong Sen, Zhong Ren-Bin, Hu Min, Chen Xiao-Xing, Zhang Ping, Zhao Tao, Liu Sheng-Gang

Chin. Phys. B . 2015, 24(7): 077302. **doi:** 10.1088/1674-1056/24/7/077302

Extraordinary optical transmission through a subwavelength composite hole-pillar array

Shao Wei-Jia, Li Wei-Min, Xu Xiao-Liang, Wang Hui-Jie, Wu Yi-Zhi, Yu Jing

Chin. Phys. B . 2014, 23(11): 117301. **doi:** 10.1088/1674-1056/23/11/117301

SPECIAL TOPIC — 80th Anniversary of Northwestern Polytechnical University (NPU)

Coupling-induced spectral splitting for plasmonic sensing with ultra-high figure of merit*

Hua Lu(陆华)†, Yi-Cun Fan(范奕村), Si-Qing Dai(戴思清), Dong Mao(毛东), Fa-Jun Xiao(肖发俊), Peng Li(李鹏), and Jian-Lin Zhao(赵建林)

MOE Key Laboratory of Material Physics and Chemistry under Extraordinary Conditions, and Shaanxi Key Laboratory of Optical Information Technology, School of Science, Northwestern Polytechnical University, Xi'an 710072, *China*

(Received 21 June 2018; revised manuscript received 7 August 2018; published online 8 October 2018)

We investigate a kind of spectral splitting effect in a plasmonic multilayer system, which consists of stacked Al_2O_3 and SiO_2 layers, a thin metal film, and a dielectric prism substrate. The results illustrate that an obvious peak appears in the center of the surface plasmon resonance (SPR)-induced reflection spectral dip in the structure with the $SiO_2/Al_2O_3/SiO_2$ layers. This spectral splitting response can be regarded as an electromagnetically induced transparency (EIT) like effect, which is attributed to the coupling and interference between the SPR on the metal film and guided-mode resonance (GMR) in the Al_2O_3 layer. The theoretical calculations agree well with the numerical simulations. It is also found that the reflection spectrum will be further split by the introduction of another Al_2O_3 layer into the multilayer structure. The reintroduced GMR in the Al_2O_3 layer changes the coupling and interference process between the SPR and GMR field, giving rise to the generation of ultra-narrow reflection dip. Especially, the spectral splitting can facilitate the realization of plasmonic sensors with ultra-high figure of merit (583), which is about 5 times larger than that of traditional SPR sensors. These results will provide a new avenue to the light field manipulation and optical functionalities, especially biochemical and environmental sensing.

Keywords: surface plasmon polaritons, multilayer, optical sensors

PACS: 73.20.Mf, 73.21.Ac, 07.07.Df **DOI:** 10.1088/1674-1056/27/11/117302

1. Introduction

Surface plasmon polaritons (SPPs) are surface electromagnetic waves coupling to collective electron oscillation and propagating along the interface between the conductor (e.g., noble metals) and dielectric material.[1,2] Nowadays, SPPs provide a significant platform for promoting the development of advanced optical physics and technologies because of their excellent capabilities of subwavelength light confinement, light field enhancement, and beyond diffraction limit.[1–5] Based on these special properties of SPPs, some novel plasmonic activities were proposed theoretically and demonstrated experimentally, such as extraordinary optical transmission,[6] optical activity,[7] nonlinear optical effect,[8] Fano resonance,[9] and electromagnetically induced transparency (EIT) like effect.[10–12] The plasmonic behaviors are also explored in new emerging materials, including grapheme,[13,14] black phosphorus,[15,16] topological insulators,[17] etc. A large number of plasmonic devices have been proposed and investigated numerically and experimentally, such as nanoscale filters,[2] all-optical switches,[18] wavelength demultiplexers,[19] solar cells,[20] logical gates,[21] modulators,[22] photodetectors,[23] waveguides,[24] and nanolasers.[25] Particularly, the applications of SPPs in optical sensors have attracted broad attention due to the high sensitivity of SPPs to the external environment.[9,26–31] Surface plasmon resonance (SPR) sensors were demonstrated for gas detection, biosensing, and refractive index measurement in the simple prism-coupling systems (e.g., Kretschmann configuration).[27,32] To improve the sensing performance, several special plasmonic responses were proposed to promote the spectral features. Fano resonance presents asymmetric spectral profile, contributing to the 7-fold improvement of the sensitivity for plasmonic sensors.[9,33] The plasmonic effect analogue to EIT in atomic systems was proposed to promote the spectral width for improving the sensitivity of sensors.[34,35] Reducing the width of resonant spectrum in SPR system is a challenge to us for the improvement of plasmonic sensing capability.

Here we propose a new plasmonic multilayer configuration consisting of stacked Al_2O_3 and SiO_2 layers, a thin metal film, and a dielectric prism substrate (Fig. 1). This Kretschmann configuration based multilayer system enables the realizing of the EIT-like spectral splitting through the coupling and interference between the SPR on the metal and GMR

*Project supported by the National Key R&D Program of China (Grant No. 2017YFA0303800), the National Natural Science Foundation of China (Grant Nos. 61705186, 11634010, and 11774290), the Natural Science Basic Research Plan in Shaanxi Province, China (Grant No. 2017JQ1023), the Technology Foundation for Selected Overseas Chinese Scholar of Shaanxi Province, China (Grant No. 2017007), and the Fundamental Research Funds for the Central Universities, China (Grant Nos. 3102018zy039 and 3102018zy050).

†Corresponding author. E-mail: hualu@nwpu.edu.cn

© 2018 Chinese Physical Society and IOP Publishing Ltd

in the Al_2O_3 layer. When another Al_2O_3 layer is coated on the multilayer structure, the induced reflection peak can be further split because of the reintroduced GMR, resulting in the ultra-narrow reflection spectral dip. It is found that the coupling-induced splitting spectrum facilitates the achievement of plasmonic sensors with an ultra-high figure of merit (FOM) of 583, which is about 5 times larger than that of traditional SPR sensors.[36] Our results will pave a new way for realizing the light manipulation and high-performance plasmonic sensing.

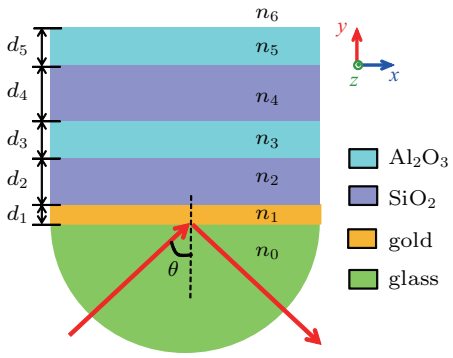


Fig. 1. (color online) Schematic diagram of the multilayer configuration with an incident angle θ of light. Here, n_0: refractive index of dielectric prism substrate, d_1 (n_1): thickness (refractive index) of gold film, d_2 (n_2): thickness (refractive index) of the first SiO_2 layer, d_3 (n_3): thickness (refractive index) of the first Al_2O_3 layer, d_4 (n_4): thickness (refractive index) of the second SiO_2 layer, d_5 (n_5): thickness (refractive index) of the second Al_2O_3 layer, and n_6: refractive index of the environment.

2. Model and theory

As shown in Fig. 1, the proposed plasmonic multilayer system is composed of stacked Al_2O_3 and SiO_2 layers, a thin metal film, and a dielectric prism substrate. The light is incident on the metal film from the glass prism with an angle θ. The metal is set to be gold, whose relative permittivity can be described by the Drude model $\varepsilon_m = \varepsilon_\infty - \omega_p^2/[\omega(j\gamma+\omega)]$,[24,37] where $\omega = 2\pi c/\lambda$ is the angular frequency of light, with c being the free-space light speed and λ the incident wavelength in vacuum. For gold, $\varepsilon_\infty = 1$, $\gamma = 2.79\times10^{13}$ rad/s, and $\omega_p = 1.3\times10^{16}$ rad/s represent the relative permittivity at the infinite frequency, electron collision frequency, and bulk plasma frequency, respectively.[37] n_0, n_1, n_2, n_3, n_4, n_5, and n_6 refer to the refractive indices of the glass prism substrate, the gold film, the first SiO_2 layer, the first Al_2O_3 layer, the second SiO_2 layer, the second Al_2O_3 layer, and the environmental surrounding, respectively. d_1, d_2, d_3, d_4, and d_5 denote the thicknesses of the gold film, the first SiO_2 layer, the first Al_2O_3 layer, the second SiO_2 layer, and the second Al_2O_3 layer, respectively. The light is incident with the transverse magnetic (TM) polarization, the spectral response of the multilayer structure can be theoretically calculated from the following equations:[32]

$$R(\theta,\lambda) = |r_{0,N}(\theta,\lambda)|^2, \tag{1}$$

$$r_{i,N}(\theta,\lambda) = \frac{r_{i,i+1}(\theta,\lambda) + r_{i+1,N}(\theta,\lambda)\exp[2jd_{i+1}k_{z,i+1}(\theta,\lambda)]}{1 + r_{i,i+1}(\theta,\lambda)r_{i+1,N}(\theta,\lambda)\exp[2jd_{i+1}k_{z,i+1}(\theta,\lambda)]}, \quad (i = N-2,\ldots,1,0), \tag{2}$$

$$r_{i,i+1}(\theta,\lambda) = \frac{\zeta_{i+1}(\theta,\lambda) - \zeta_i(\theta,\lambda)}{\zeta_{i+1}(\theta,\lambda) + \zeta_i(\theta,\lambda)}, \quad (i = 0,1,\ldots,N-1), \tag{3}$$

$$k_{z,i}(\theta,\lambda) = \frac{2\pi}{\lambda}\sqrt{n_i^2 - \varepsilon_0\sin^2\theta}, \quad (i = 0,1,\ldots,N), \tag{4}$$

$$\zeta_i(\theta,\lambda) = \frac{n_i^2}{k_{z,i}(\theta,\lambda)}, \quad (i = 0,1,\ldots,N), \tag{5}$$

where $r_{i,i+1}$ is the reflection coefficient of light propagation at the interface between the adjacent layers i and $i+1$ ($i = 0, 1, \ldots, N-1$), N is the number of layers in the multilayer structure, and $k_{z,i}$ denotes the wavevector of the light propagation along the x-axis direction in the optical layer i ($i = 0, 1, \ldots, N$). Using Eqs. (1)–(5), we can theoretically calculate the evolution of reflection spectrum with d_3 in the multilayer structure with $\theta = 80°$, $d_1 = 60$ nm, $d_2 = 2.0$ μm, $d_4 = 2.0$ μm, $d_5 = 0$ μm, which is shown in Fig. 2(a). Here, the refractive indices are set to be $n_0 = 1.516$, $n_1 = (\varepsilon_m)^{1/2}$, $n_2 = 1.45$, $n_3 = 1.76$, $n_4 = 1.45$, $n_5 = 1.76$, and $n_6 = 1$. In Fig. 2(b), we can see that there exists an obvious dip in the reflection spectrum when $d_3 = 0$ μm. To verify the theoretical calculations, we numerically simulate the spectral response and field distributions in the structure by using the finite-difference time-domain

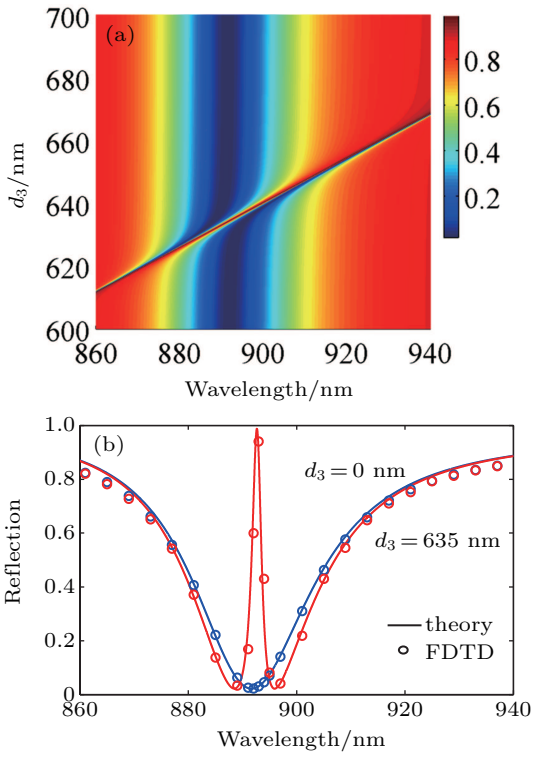


Fig. 2. (color online) (a) Evolution of reflection spectrum with the Al_2O_3 thickness d_3. (b) Reflection spectra of the multilayer structure with $d_3 = 0$ nm and 635 nm. The other parameters are set to be $\theta = 80°$, $d_1 = 60$ nm, $d_2 = 2.0$ μm, $d_4 = 2.0$ μm, $d_5 = 0$ μm, and $n_6 = 1$.

(FDTD) method. In this method, the perfectly matched layer (PML) absorbing boundary conditions and Bloch boundary conditions (BBC) are set at the top/bottom and right/left sides of the computational space, respectively.[38] The FDTD simulations are in excellent agreement with the theoretical results.

3. Results and analysis

The reflection dip is generated at a wavelength of 893 nm, where the SPR on the metal satisfies the wavevector matching condition with incident light being in the prism, namely, $k_0 n_{spp} = k \sin\theta n_0$.[39,40] At this wavelength, the SPR is excited on the metal film as shown in Fig. 3(a). In Fig. 2(a), we can observe that the distinct peaks appear in the broad reflection spectral dip when d_3 approaches to special values. For instance, a narrow reflection peak can be generated at the wavelength of 893 nm ($\lambda = 893$ nm) when $d_3 = 635$ nm as depicted in Fig. 2(b). At this wavelength, the GMR can be generated in the high-refractive index (Al_2O_3) layer, as shown in Fig. 3(b). This optical phenomenon is analogous to the EIT effect in an atomic system.[41] Here, the SPR can be regarded as the excitation state $|1\rangle$, the GMR can be analogy to the excitation state $|2\rangle$, the light is incident on the metal film and generates SPR, which can be analogue to the transition process from ground state $|0\rangle$ to $|1\rangle$. The incident light cannot directly excite the GMR in the Al_2O_3 layer, which denotes that the transition process from $|0\rangle$ to $|2\rangle$ is not allowed. The GMR is generated via the coupling of SPR evanescent field, corresponding to the transition between $|1\rangle$ and $|2\rangle$. Thus, the two possible pathways $|0\rangle \rightarrow |1\rangle$ and $|0\rangle \rightarrow |1\rangle \rightarrow |2\rangle \rightarrow |1\rangle$ will generate the destructive interference, giving rise to the weakness of SPR field and the spectral splitting. The EIT-like effect is derived from the excitation of dark mode (GMR in the Al_2O_3 layer) induced by the coupling of bright modes (SPR on the metal).[42,43] The coupling becomes weaker with increasing d_2, resulting in the narrower width and lower height of the EIT-like spectral peak.[11,41] As shown in Fig. 2(a), the induced reflection peak shows a redshift with the increase of d_3 due to the redshift of resonant wavelength for the Al_2O_3 layer.

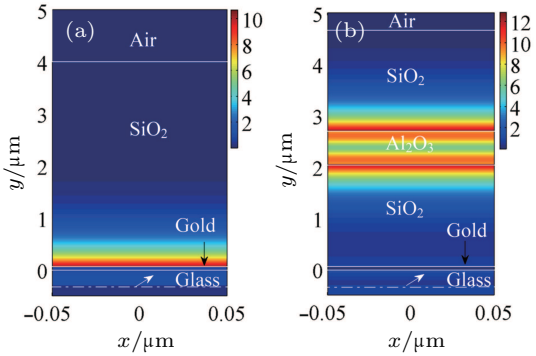


Fig. 3. (color online) Electric field distribution of $|E|$ at $\lambda = 893$ nm in the multilayer structure (a) without and (b) with the first Al_2O_3 layer (i.e., $d_3 = 0$ and 635 nm).

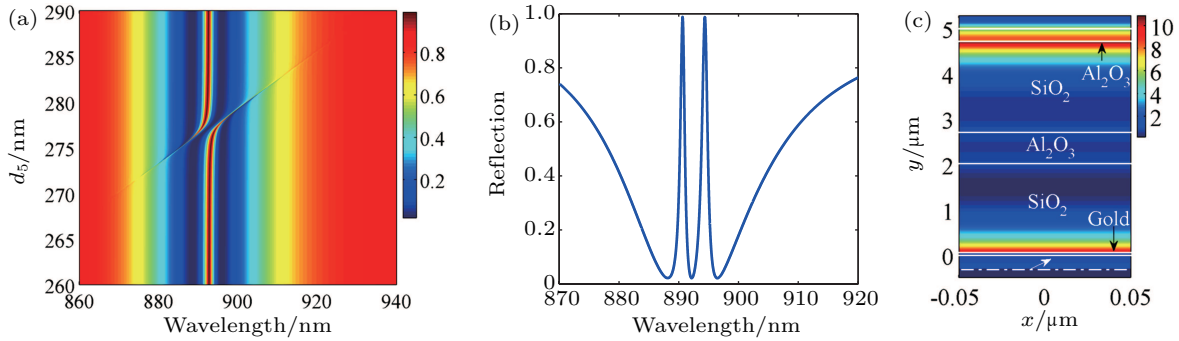


Fig. 4. (color online) (a) Evolution of reflection spectrum with the thickness of the second Al_2O_3 layer d_5. (b) Reflection spectrum of the multilayer structure with $d_5 = 277$ nm. (c) Electric field distribution of $|E|$ at reflection dip ($\lambda = 892.3$ nm) in panel (b). Here, $\theta = 80°$, $d_1 = 60$ nm, $d_2 = 2.0$ μm, $d_3 = 635$ nm, $d_4 = 2.0$ μm, and $n_6 = 1$.

Subsequently, we investigate the evolution of reflection spectrum with d_5 in the multilayer structure with $\theta = 80°$, $d_1 = 60$ nm, $d_2 = 2.0$ μm, $d_3 = 635$ nm, and $d_4 = 2.0$ μm. We can see in Fig. 4(a) that the reflection spectral peak can be further split when d_5 reaches a particular value. Figure 4(b) shows the reflection spectral response in the multilayer structure with $d_5 = 277$ nm. A sharp spectral dip can be generated in the EIT-like reflection peak at a wavelength of 892.3 nm. By the FDTD method, we numerically simulate the electric field distribution of the multilayer system at the wavelength of 892.3 nm and the results are shown in Fig. 4(c). It is found that the GMR in the second Al_2O_3 layer is excited, and the GMR in the first Al_2O_3 layer disappears. The successive spectral splitting can be attributed to the coupling and interference between the GMR in Al_2O_3 layers and SPR on the metal film. This interesting spectral response can also be explained according to the EIT-like theoretical mechanism. The introduction of the GMR into the second Al_2O_3 layer provides another excitation state $|3\rangle$, giving rise to the generation of new coupling (transition) and interference processes. Here, the GMR in the second Al_2O_3 layer can only effectively couple with the GMR in the first Al_2O_3 layer. Thus, the transition from $|1\rangle$ to $|3\rangle$ is

forbidden. The two possible pathways $|0\rangle \rightarrow |1\rangle \rightarrow |2\rangle$ and $|0\rangle \rightarrow |1\rangle \rightarrow |2\rangle \rightarrow |3\rangle \rightarrow |2\rangle$ will form destructive interference, resulting in the disappearing of electrical field in the first Al_2O_3 layer, which is shown in Fig. 4(c). Meanwhile, the disappearance of the electric field in the first Al_2O_3 layer prevents the transition from $|2\rangle$ to $|1\rangle$. Thus, the SPR field still exists on the metal film. As shown in Fig. 4(a), the splitting spectral dip has a redshift with the increase of d_5, which is attributed to the redshift of resonant wavelength of GMR in the second Al_2O_3 layer. This spectral splitting response contributes to the narrower SPR resonant spectrum, providing a new pathway toward the realization of high-performance plasmonic sensing.

Next, we study the influence of the thickness of the second SiO_2 layer d_4 on the splitting of reflection spectrum. As shown in Fig. 5, the reflection dip in the center of the spectral peak becomes narrower with increasing d_4. This spectral response results from the gradual weakening of optical coupling between the first and the second Al_2O_3 layers with the increase of d_4.[11] For example, the spectral full-width at half-maximum (FWHM) of the reflection dip can reach 0.6 nm when $d_4 = 2.5$ μm, which is about 20 times smaller than the SPR spectral width. In order to explore the sensing features based on this spectral splitting effect, we investigate the spectral response in this multilayer structure with different surrounding refractive indices. The reflection dip shows a redshift with increasing n_6, while the position of the reflection peak does not change. This is due to the fact that the wavelength of GMR in the second Al_2O_3 layer increases with n_6, while the reflection peak is not sensitive to the change of n_6. As shown in Fig. 6(a), the reflection spectrum can approach a maximum value from the minimum value (spectral dip) when n_6 changes from 1 to 1.003. The sensitivity ($S = \Delta\lambda/\Delta n$) of the refractive index sensing is about 350 nm/RIU. Thus, the figure of merit (FOM = S/FWHM) as a critical sensing factor can reach as high as 583, which is about 5 times larger than that of traditional Kretschmann configuration SPR sensors.[36] The FOM is also two orders of magnitude larger than that of plasmonic sensing based on the EIT-like effect in planar metamaterials.[34] To contain the information about the relative intensity change, the FOM* was proposed by Becker *et al.* for the measurement of optical sensing features, which is defined as $\text{FOM}^* = \max[\mathrm{d}I/I\mathrm{d}n]$. Here, I and $\mathrm{d}I$ denote the reflection intensity and its variation under the condition of the refractive index change $\mathrm{d}n$, respectively.[44] The results in Fig. 6(b) show that the FOM* based on the spectral splitting in the multilayer system can approach 1.46×10^4, which is 29 times larger than our result reported previously in plasmonic waveguides.[9] The splitting spectrum and FOM* are dependent on the gold layer thickness d_1. More specifically, when d_1 decreases, the reflection dip of the splitting spectrum will become much shallower and the FOM* will decrease (not shown here). When another Al_2O_3 layer is introduced into the structure, the reflection spectrum can be further split and generate a narrower spectral peak.

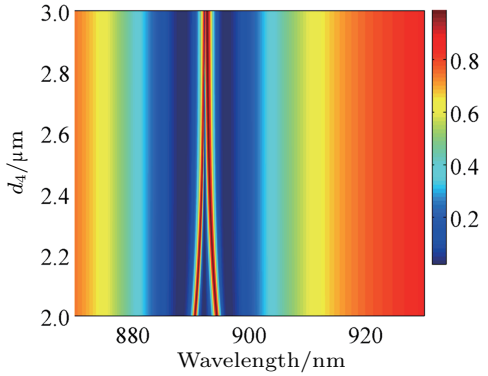


Fig. 5. (color online) Evolution of reflection spectrum with the thickness of the second SiO_2 layer d_4 when $n_6 = 1$. Here, $\theta = 80°$, $d_1 = 60$ nm, $d_2 = 2.0$ μm, $d_3 = 635$ nm, and $d_5 = 277$ nm.

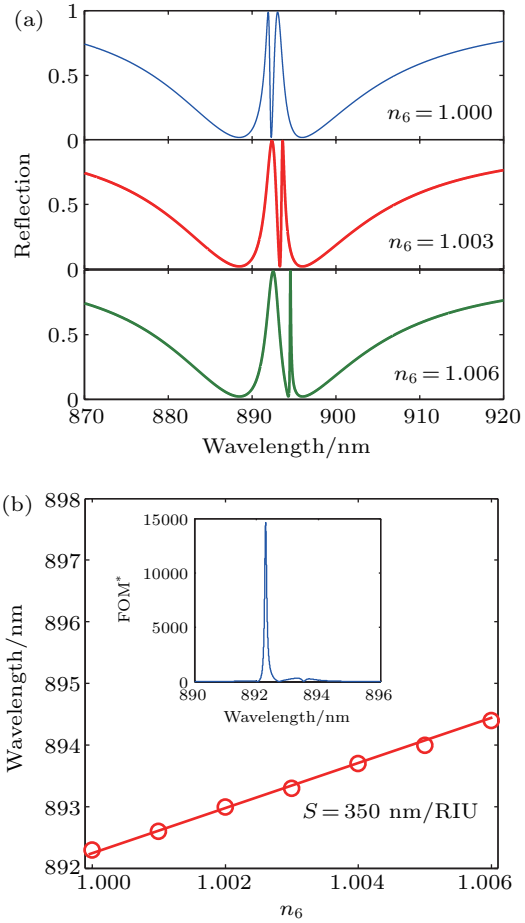


Fig. 6. (color online) (a) Reflection spectra of the multilayer structure with different n_6. (b) Reflection dip positions with different values of surrounding refractive index n_6. Inset shows figure of merit (FOM*) of plasmonic sensing. Here, $\theta = 80°$, $d_1 = 60$ nm, $d_2 = 2.0$ μm, $d_3 = 635$ nm, $d_4 = 2.5$ μm, and $d_5 = 277$ nm.

4. Conclusions and perspectives

We have theoretically and numerically investigated the generation and application of EIT-like spectral splitting effect in a plasmonic multilayer configuration consisting of a

thin gold film on a glass prism substrate (Kretschmann configuration) and stacked Al_2O_3/SiO_2 layers. The results show that the SPR-induced spectral dip can be split and generate a narrow EIT-like peak due to the coupling and interference between the SPR on the metal film and the GMR in the Al_2O_3 layer. The theoretical calculations agree well with the numerical simulations. Especially, we find that the EIT-like induced reflection peak can be further split when another Al_2O_3 layer is introduced into the multilayer structure. This successive spectral splitting response can also be explained from the EIT-like coupling mechanism. By means of the spectral splitting, the ultra-narrow reflection dip with a spectral width of 0.6 nm can be achieved, which contributes to the realization of plasmonic sensors with the ultra-high FOM. The FOM can approach to 583, which is about 5 times larger than that of traditional Kretschmann configuration SPR sensors. The plasmonic spectral response in the proposed multilayer system will pave a new way for the light manipulation and the improvement of optical functionalities, especially biochemical and environmental sensing.

References

[1] Gramotnev D and Bozhevolnyi S 2010 *Nat. Photon.* **4** 83
[2] Lu H, Liu X, Mao D, Wang L and Gong Y 2010 *Opt. Express* **18** 17922
[3] Min C, Shen Z, Shen J, Zhang Y, Fang H, Yuan G, Du L, Zhu S, Lei T and Yuan X 2013 *Nat. Commun.* **4** 2891
[4] Lu H, Mao D, Zeng C, Xiao F, Yang D, Mei T and Zhao J 2018 *Opt. Mater. Express* **8** 1058
[5] Lu H, Gan X, Mao D and Zhao J 2017 *Photon. Res.* **5** 162
[6] Liu H and Lalanne P 2008 *Nature* **452** 728
[7] Yu P, Li J, Tang C, Cheng H, Liu Z, Li Z, Liu Z, Gu C, Li J, Chen S and Tian J 2016 *Light Sci. Appl.* **5** e16096
[8] Kauranen M and Zayats A V 2012 *Nat. Photon.* **6** 737
[9] Lu H, Liu X, Mao D and Wang G 2012 *Opt. Lett.* **37** 3780
[10] Liu N, Weiss T, Mesch M, Langguth L, Eigenthaler U, Hirscher M, Sönnichsen C and Giessen H 2010 *Nano Lett.* **10** 1103
[11] Lu H, Gan X, Mao D, Jia B and Zhao J 2018 *Sci. Rep.* **8** 1558
[12] Zhou W, Wang X and Wang J 2015 *J. Mod. Opt.* **62** 1027
[13] Luo W, Cai W, Wu W, Xiang Y, Ren M, Zhang X and Xu J 2016 *2D Mater.* **3** 045001
[14] Lu H, Zeng C, Zhang Q, Liu X, Hossain M, Reineck P and Gu M 2015 *Sci. Rep.* **5** 8443
[15] Liu Z and Aydin K 2016 *Nano Lett.* **16** 3457
[16] Lu H, Gong Y, Mao D, Gan X and Zhao J 2017 *Opt. Express* **25** 5255
[17] Yue Z, Cai B, Wang L, Wang X and Gu M 2016 *Sci. Adv.* **2** e1501536
[18] Min C, Wang P, Chen C, Deng Y, Lu Y, Ming H, Ning T, Zhou Y and Yang G 2008 *Opt. Lett.* **33** 869
[19] Lu H, Liu X, Gong Y, Mao D and Wang L 2011 *Opt. Express* **19** 12885
[20] Zhang Y, Du Y, Shum C, Cai B, Le N, Chen X, Bradbury G, Duck B, Fell C, Zhu Y and Gu M 2016 *Sci. Rep.* **6** 24972
[21] Yang X, Hu X, Yang H and Gong Q 2017 *Nanophoton.* **6** 365
[22] Dennis B, Haftel M, Czaplewski D, Lopez D, lumberg G and Aksyuk A 2015 *Nat. Photon.* **9** 267
[23] Lu H and Gu M 2017 *Appl. Phys. B* **123** 71
[24] Lu H, Liu X and Mao D 2012 *Phys. Rev. A* **85** 053803
[25] Oulton R, Sorger V, Zentgraf T, Ma R, Gladden C, Dai L, Bartal G and Zhang X 2009 *Nature* **461** 629
[26] Liedberg B, Nylander C and Lundstro¨m I 1983 *Sens. Actuators* **4** 299
[27] Zhang J, Dai S, Ma C, Di J and Zhao J 2017 *Opt. Lett.* **42** 3462
[28] Wang J, Fan C, He J, Ding P, Liang E and Xue Q 2013 *Opt. Express* **21** 2236
[29] Wang J, Liu X, Li L, He J, Fan C, Tian Y, Ding P, Chen D, Xue Q and Liang E 2013 *J. Opt.* **15** 105003
[30] Wang J, Mu K, Ma F, Zang H, Fan C, He J, Liang E and Ding P 2015 *Opt. Commun.* **338** 399
[31] Yuan B, Zhou W and Wang J 2014 *J. Opt.* **16** 105013
[32] Xiao C and Sui S 2000 *Sens. Actuators B* **66** 174
[33] Zhan Y, Lei D Y, Li X and Maier S 2014 *Nanoscale* **6** 4705
[34] Liu N, Weiss T, Mesch M, Langguth L, Eigenthaler U, Hirscher M, Sönnichsen C and Giessen H 2010 *Nano Lett.* **10** 1103
[35] He X, Wang L, Wang J, Tian X, Jiang J and Geng Z 2013 *J. Phys. D: Appl. Phys.* **46** 365302
[36] Blaber M, Arnold M and Ford M 2009 *J. Phys. Chem. C* **113** 3041
[37] Taflove A and Hagness S 2000 *Computational Electrodynamics: The Finite-Difference Time-Domain Method* (2nd Edn.) (Boston: Artech House)
[38] Lu H, Liu X, Mao D, Gong Y and Wang G 2011 *Opt. Lett.* **36** 3233
[39] Wang J, Zhang J, Tian Y, Fan C, Mu K, Chen S, Ding P and Liang E 2017 *Opt. Express* **25** 497
[40] Elshorbagy M, Cuadrado A and Alda J 2017 *Photon. Res.* **5** 654
[41] Roh S, Chung T and Lee B 2011 *Sensors* **11** 1565
[42] Wang J, Zhang J, Fan C, Mu K, Liang E and Ding P 2017 *Opt. Commun.* **383** 36
[43] Wang J, Yuan B, Fan C, He J, Ding P, Xue Q and Liang E 2013 *Opt. Express* **21** 25159
[44] Becker J, Truegler A, Jakab A, Hohenester U and Soennichsen C 2010 *Plasmonics* **5** 161